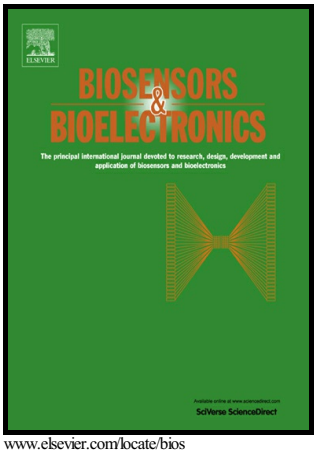

www.elsevier.com/locate/bios

Electroactive crown ester-Cu^{2+} complex with in-situ modification at molecular beacon probe serving as a facile electrochemical DNA biosensor for the detection of CaMV 35s

Fengping Zhan, Xiaolei Liao, Feng Gao, Weiwei Qiu, Qingxiang Wang

PII: S0956-5663(16)31070-3
DOI: http://dx.doi.org/10.1016/j.bios.2016.10.055
Reference: BIOS9277

To appear in: *Biosensors and Bioelectronic*

Received date: 2 August 2016
Revised date: 10 October 2016
Accepted date: 19 October 2016

Cite this article as: Fengping Zhan, Xiaolei Liao, Feng Gao, Weiwei Qiu and Qingxiang Wang, Electroactive crown ester-Cu^{2+} complex with in-situ modification at molecular beacon probe serving as a facile electrochemical DNA biosensor for the detection of CaMV 35s, *Biosensors and Bioelectronic* http://dx.doi.org/10.1016/j.bios.2016.10.055

Electroactive crown ester-Cu^{2+} complex with in-situ modification at molecular beacon probe serving as a facile electrochemical DNA biosensor for the detection of CaMV 35s

Fengping Zhan, Xiaolei Liao, Feng Gao, Weiwei Qiu, Qingxiang Wang*

College of Chemistry and Environment, Fujian Province Key Laboratory of Morden Analytical Science and Separation Technology, Minnan Normal University, Zhangzhou 363000, P. R. China

Submitted to **Biosensors and Bioelectronics**

Prof. Qingxiang Wang

Tel: +86-596-2596780;

Fax: +86-596-2527801;

E-mail: axiang236@126.com.

Abstract

A novel electrochemical DNA biosensor has been facilely constructed by in-situ assembly of electroactive 4'-aminobenzo-18-crown-6-copper(Ⅱ) complex (AbC-Cu^{2+}) on the free terminal of the hairpin-structured molecule beacon. The 3'-SH modified molecule beacon probe was first immobilized on the gold electrode (AuE) surface through self-assembly chemistry of Au-S bond. Then the crow ester of AbC was covalently coupled with 5'–COOH on the molecule beacon, and served as a platform to attach the Cu^{2+} by coordination with ether bond (–O–) of the crown cycle. Thus, an electroactive molecule beacon-based biosensing interface was constructed. In comparison with conventional methods for preparation of electroactive molecule beacon, the approach presented in this work is much simpler, reagent- and labor-saving. Selectivity study shows that the in-situ fabricated electroactive molecule beacon remains excellent recognition ability of pristine molecule beacon probe to well differentiate various DNA fragments. The target DNA can be quantatively determined over the range from 0.10 pM to 0.50 nM. The detection limit of 0.060 pM was estimated based on signal-to-noise ratio of 3. When the biosensor was applied for the detection cauliflower mosaic virus 35s (CaMV 35s) in soybean extraction samples, satisfactory results are achieved. This work opens a new strategy for facilely fabricating electrochemical sensing interface, which also shows great potential in aptasensor and immurosensor fabrication.

Keywords

In-situ modification;
Electrochemical DNA sensor;
4'-aminobenzo-18-crown-6;
Copper complex;
Molecule beacon.

1. Introduction

Along with the quick development of transgenic technology, more and more transgenic products have entered into people's daily lives. However, the risk of transgenic products to the environment, ecosystem, and human body's health is still unclear, which makes it of great importance to develop reliable methods for fast and accurate detection of specific transgenic sequences (Manzanares-Palenzuela et al., 2015; Fu et al. 2016). The electrochemical DNA (E-DNA) biosensors, in comparison with the traditional approaches such as polymerase chain reaction (PCR) (Obradovic et al. 2016), fluorescence in-situ hybridization (Wang et al. 2016) and flow cytometry (Nowicka et al. 2016), own considerable superiorities such as easy operation, high sensitivity, outstanding accuracy, low cost and simple equipment. Up to date, lots of efforts have been made to construct E-DNA biosensors for monitoring transgenetic products by detecting the specific DNA sequences such as cauliflower mosaic virus 35s (CaMV 35s), nopaline synthase (NOS), phosphinothricin acetyltransferase (PAT) etc. But, the common approach to convert the hybridization event to the readable signal in these E-DNA biosensors relies on the use of external electroactive hybridization indicators (Alves-Balvedi et al. 2016; Zheng et al. 2014), which involves fussy indicators binding/rinsing process during each hybridization step, making the detection process time-consuming and laborious. In addition, the non-specific adsorption of the indicators on single-stranded usually causes large background response, which decreases the accuracy and sensitivity of the biosensor.

Molecular beacon (MB) with functional molecules tagged at 3'-end and 5'-end is a class of nucleic acid probes with unique loop-stem structure, which has been applied for real-time quantitative nucleic acid analysis, bioimaging and therapy (Zheng et al. 2016). In 2003, Fan et al. (Fan et al. 2003) firstly proposed the combination of MB technology and electrochemistry, and developed a novel E-DNA sensor. As the electrode-confined MB is hybrized with target DNA, the stem-loop structure of the probe will be opened and transfer to rigid DNA duplex. Thus, the signal tags are driven away from the electrode surface, causing the attenuation of the signal, reaching the aim of target DNA analysis. Methylene blue (MTB) (Tyagi et al. 1998; Yang et al. 2012) and ferrocene (Fc) (Chatelain et al. 2012; Fan et al. 2003; Yang et al. 2012) are the most used electroactive tags due to their excellent electrochemical response. However, the relative insufficiency in types of the two electrochemical tags hinders the development of the versatile MB-based chips for high-throughput detection of

multiple analytes. On the other hand, the relatively inferior chemical stability of MTB and Fc also decreases the durability and using life of the biosensors. In addition, the conventional preparation methods of the electroactive MBs that based on liquid-phase synthesis, separation and purification are time- and reagent- consuming. Thus, it is still of urgent demand to explore new tags and facile synthesis method of electroactive MBs for the detection of specific sequences.

Transition metal complex has the advantages of low toxity, easy-for-preparation, excellent chemical stability, intense redox signal, and high structure flexibility. Based on these merits, the metal-based complexes have been frequently designed and utilized as electrochemical DNA hybridization indicators (Wang et al. 1996; Wang et al. 2013). However, the use of metal complex as the electroactive tag for MB is scarcely reported. Copper ion (Cu^{2+}) is a relatively inexpensive, chemically stable and low toxicity transition metal ion. In electrochemical aspect, it shows moderate redox potential, high electron transfer reversibility (Cu(II)/Cu(I) couple) and strong response signal. Therefore, it was often selected as an electrochemical signal resource to bind to some functional ligand, and then be used as electrochemical probe for biosensing application (Chen et al. 2015; Drewry et al. 2011; Sharma et al. 2017).

Crown ethers have the excellent ability for selective complexation with metal ions, and thus often being used as functional material for selective determination of various metal ions (James et al. 2004; Park et al. 2010). 18-crown-6 is important host crow ether, of which the cavity size is comparable to the size of a range of the metal ions to form stable “metal-in-cavity” type complexes in solution and the solid state (Gokel et al. 2004; Wang et al. 2015). Inspired by these characteristics, a novel biosensing interface through stepwise *in-situ* grafting of AbC and Cu^{2+} on the free terminal of hairpin-structured MB was proposed (Fig. 1): The probe DNA with 5′-COOH and 3′-SH was first immobilized on AuE through Au-S bond, then the AbC and Cu^{2+} were sequentially modified 5′-COOH successively via covalent and coordinative chemistry, respectively. Due to the unique stem-loop structure of the MB probe, the modified electroactive AbC-Cu^{2+} tag is close to the electrode surface under its initial situation, resulting in an extremely large electrochemical signal of the probe electrode. Upon hybridization, the stem-loop structure was opened and changed to the rigid linear structure, from which the electroactive AbC-Cu^{2+} was driven away from electrode surface, leading to decrease of the redox signal of the biosensor. Thus the hybridization event happened on the electrode surface can be effectively monitored.

In comparison with conventional methods for fabricating the electroactive MB probes, the *in-situ* assembly approach presented in this work avoids the complicated processes including homogeneous reaction, separation and purification, making the fabrication much simpler, reagent-saving and labor-saving. Meanwhile, as an inorganic electroactive tag, the AbC-Cu^{2+} complex can effectively enhances the stability of the sensor. The presented approach also opens a new strategy for the fabrication of novel electrochemical biosensing interface.

<Fig. 1 >

2. Experimental

2.1 Reagents and apparatus

4'-aminobenzo-18-crown-6 (AbC) and Tris (2-carboxyethyl) phosphine hydrochloride (TCEP) were purchased from Sigma-Aldrich (China). Tris (hydroxy-methyl) aminomethane (Tris) was provided by Sinopharm Chemical Reagent Co., Ltd (China). N,N'-dicyclohexylcarbodiimide (DCC) was obtained from TCI Development Co. Ltd (China). Ethylenediaminetetraacetic acid (EDTA) and N,N'-dimethylformamide (DMF) were purchased from Xilong Chemical Co., Ltd (China). Nickel chloride hexahydrate ($NiCl_2 \cdot 6H_2O$), cobalt(II) acetate tetrahydrate ($Co(CH_3COO)_2 \cdot 4H_2O$), manganese sulfate monohydrate ($MnSO_4 \cdot H_2O$), samarium(III) nitrate hexahydrate ($Sm(NO_3)_3 \cdot 6H_2O$), iron chloride hexahydrate ($FeCl_3 \cdot 6H_2O$) and copper nitrate trihydrate ($Cu(NO_3)_2 \cdot 3H_2O$) were supplied by Aladdin Reagent (China). All the chemicals were of analytical reagent grade and used without further purification. Double-distilled water (DDW) was used throughout the experiments.

The oligonucleotides related to CaMV 35s promoter gene were provided by Shanghai Sangon Biotechnology Co., Ltd (China). Their base sequences with the modified groups are displayed as follows:

• MB probe sequence with bifunctional groups (S1): 5'-COOH- GC GAG TCT TTG GGA CCA CTG TCG CTC GC- $(CH_2)_6$-SH-3'

•Complementary sequence (S2): 5'-CGA CAG TGG TCC CAA AGA-3'

•One-base mismatched sequence (S3): 5'-CGA CAG TGG TCC CAA CGA-3'

•Non-complementary sequence (S4): 5'-GCA TCG AGC GAG CAG GTA-3'

The MB probe solution was prepared by dissolving appropriate probe DNA (S1) in 1 mL immobilization buffer (pH 8.0) that prepared by 10.0 mM $MgCl_2$, 10.0 mM TCEP, 25 mM Tris, and 25 mM EDTA. The hybridization and electrode washing

buffer were 10.0 mM phosphate buffer saline (PBS, pH 6.8) with 25.0 mM KCl and 0.10 M $MgCl_2$. The supporting electrolyte solution for the electrochemical measurements was 0.10 M borate buffer saline with 5% (*V*/*V*) ethanol, 25.0 mM KCl and 0.10 M $MgCl_2$. A CHI 650C electrochemical analyzer (China) was used for all the electrochemical measurements including cyclic voltammetry (CV), electrochemical impedance spectroscopy (EIS) and differential pulse voltammetry (DPV). A conventional three-electrode system, consisting of a bare or modified gold disk (Φ = 2.0 mm) as working electrode, a platinum wire as auxiliary electrode and an Ag/AgCl (3.0 M KCl) as reference electrode, was used for electrochemical measurements. Attenuated total reflection infrared spectra (ATR-IR) were recorded on a NICOLET iS 10 spectrometer (USA).

2.2 Preparation of the biosensor

For the effective modification of the Au electrode (AuE), it is necessary to clean the electrode through several steps: first, in order to remove the solid pollutants adsorbed on the electrode surface, the bare AuE was mechanically polished with 1.0 μm, 0.3 μm and 0.05 μm α-Al_2O_3, in turn, and then sequential ultrasonic washing in DDW, DDW/ethanol mixture (*V*/*V*=1:1) and DDW. Then, the electrode was immersed in strongly oxidizing Piranha solution (H_2SO_4/H_2O_2, *V*/*V*=7:3) for 20 min to remove the adsorbed organic pollutants. Finally, the electrode was circularly swept in 0.5 M H_2SO_4 from 1.5 to −0.2 V with the scan rate of 100 mV s^{-1} until constant CV curves were achieved, from which the oxide film on the electrode can be effectively eliminated to be beneficial for following assembly modification. Whereafter, the cleaned AuE was immersed into 10 nM probe MB solution for 20 h at 4 °C to achieve probe DNA modified electrode (S1/AuE) through Au-S assembly chemistry. Then, the AbC was covalently grafted on 5'-end of S1 through immersing S1/AuE into 2 mL DMF containing 1 mM DCC and 10 μM AbC for 12 h at 4 °C. The modified electrode was denoted as AbC-S1/AuE. For assembly of electroactive Cu^{2+}, the AbC-S1/AuE was incubated in 6.0 mM $Cu(NO_3)_2$ for 30 min under gentle stirring, through which the Cu^{2+} ions were in-situ attached on the sensing interface through coordination with AbC. After washing with PBS, the biosensing interface of Cu^{2+}-AbC-S1/AuE was achieved.

2.3 Hybridization procedures

The hybridization reaction was performed by incubating Cu^{2+}-AbC-S1/AuE in

hybridization buffer containing desired concentration of target DNA (S2) for 45 min at 37 °C. Afterwards, the electrode was washed with blank hybridization buffer and DDW to remove the unhybridized DNA. The hybridized electrode was denoted as Cu^{2+}-AbC-S2-S1/AuE. The hybridization of the Cu^{2+}-AbC-S1/AuE with the one-base mismatched DNA (S3) and the noncomplementary DNA (S4) were performed through the similar procedures. The obtained electrodes were denoted as Cu^{2+}-AbC- S3-S1/AuE and Cu^{2+}-AbC-S4-S1/AuE, respectively.

2.4 Electrochemical characterization and measurements

The fabrication process of the DNA biosensor was electrochemically characterized through CV and EIS in 1.0 mM $[Fe(CN)_6]^{3-/4-}$ solution containing 0.1 M KCl. The CV was recorded within the potential ranging from –0.2 V to 0.6 V with the scan rate of 100 mV s^{-1}. EIS was collected in the frequency range from 1 Hz to 10^5 Hz at an applied potential of 203 mV, which is the formal potential of the CV test (Diao et al. 2000, Tabrizi et al. 2015, Yılmaz et al. 2016). The electrochemical behaviors and the hybridization monitoring of the developed biosensor were carried out through CV and DPV technologies in supporting electrolyte. The CV was scanned within the potential range from –0.2 V to 0.6 V. DPV was obtained in the potential range from –0.2 V to 0.6 V with an increment potential of 0.004 V, pulse width of 0.05 s, pulse amplitude of 0.05 V, pulse period of 0.2 s, sample width of 0.0167 s and quiet time of 2 s.

2.5 Preparation of real samples

To prepare the real samples, the DNA from the market-purchased soybean was extracted by the CTAB method (Lipp et al. 1999; Malothu et al. 2016). Then, the obtained DNA was digested by the following procedure: adding 16 μL DDW, 2 μL TE buffer (pH=8.0) and 1 μL ice-colded restriction enzyme Hind III into 1 μL 0.5 μg μL^{-1} extracted DNA, to prepare the digestion mixture solution. Followed by reaction in water bath (37 °C) for 60 min, the mixture was further heated at 80 °C for 20 min to devitalize the enzyme. Furthermore, the DNA in the mixture was denatured in water-bath (100 °C) for 5 min, and then diluted 10 times with hybridization buffer for the following test.

3. Results and Discussion

3.1 ATR-FTIR and electrochemical characterization on grafing of AbC on probe DNA

ATR-FTIR technique is a convenient, non-destructive and reliable tool to probe

the adsorption of organic or biological molecules on a solid surface (Giambattista et al. 2011; Mircescu et al. 2012). Fig. 2 shows the ATR-FTIR results of the AuE upon assembly with probe DNA (S1) and in-situ modification of AbC. As seen, the bare AuE does not produce any significant absorption band in wavenumber range from 4000 to 500 cm^{-1} (curve a), showing that the bare AuE had been sufficiently cleaned. After S1 was self-asemblied onto AuE through Au-S bond (curve b), it is found that the ATR-FTIR spectrum changes significantly, and the newly emerged bands can be well assigned to the characteristic absorption of DNA (Banyay et al. 2003; Cui et al. 2015). The broad absorption band ascribed to the O-H stretching vibration of DNA phosphate backbone appears at 3383 cm^{-1}. Two small adjacent peaks in the range of 3000~2800 cm^{-1} relate to the asymmetric and symmetric stretching vibrations of $–CH_2–$ in the DNA's sugar- phosphate backbone. The strong sharp peak at 1604 cm^{-1} exhibits the typical absorption feature of –C=O, which may be the vibration absorption from the base of DNA and –COOH on 5'-end. The bands located at 1417 cm^{-1} and 1328 cm^{-1} are to the characteristic peaks of DNA's base-sugar entities. The 1068 cm^{-1} and 934 cm^{-1} bands are to the P–O stretching vibration of P–O–C groups. All these results highlight that S1 probe have been successfully assembled on the AuE surface. After S1/AuE was reacted with AbC using DCC as the crosslinker, it is observed that the bands at 2926 cm^{-1} and 2852 cm^{-1} corresponding to the asymmetric and symmetric stretching vibrations of $–CH_2$ enhance greatly, which can be ascribed to the increase of $–CH_2$ group from crown ether. The peaks at 1653 cm^{-1}, 1520 cm^{-1} and 1298 cm^{-1} are related to the bending vibration of –NH, and the stretching vibration of –CN– in the formed amide unit. The strong peak at 1047 cm^{-1} can be assigned to the stretching vibration of C–O–C groups of the crown ether backbone. These new bands also confirm that AbC have been anchored to S1 through the condensation reaction between –COOH group at 5′-end of MB probe and the $–NH_2$ of AbC.

<Fig. 2 >

The stepwise modification processes of S1 and AbC on the AuE were also investigated by electrochemical method using $[Fe(CN)_6]^{3-/4-}$ as electrochemical probe. The corresponding CV and EIS results and the related discussion are given in Supplementary Information (Fig. S1). The results also demonstrate that probe DNA and the functional platform of AbC had been immobilized on AuE as expected.

3.2 Coordination assembly of Cu^{2+} on AbC-S1/AuE and its electrochemical behavious

It has been reported that the crown ether cycle has the function to capture metal ion through coordination reaction (Mehta et al. 2014; Gokel et al. 2004; Wang et al. 2015). Therefore in this work, in order to obtain the electroactive sensing interface, the AbC was applied as the capture platform for the electroactive ions. Fig. 3A shows the CVs of AbC-S1/AuE before (a) and after interaction with Cu^{2+}. Obviously, there is not any Faradic electrochemical response for the AbC-S1/AuE in the potential range from –0.2 V to +0.6 V (curve a), suggesting that the assembled AbC-S1 layer is electro-inactive under the measured conditions. Nevertheless, after the AbC-S1/AuE was incubated in 6.0 mM $Cu(NO_3)_2$ solution for 30 min and then tested under the same conditions, a pair of intense redox peaks appear at +0.32 V and +0.21 V (curve c), which is in good consistence with the electron transfer process of the Cu^{2+}/Cu^{+} couple in literatures (Chen et al. 2015; Wang et al. 2016). In order to investigate the contribution of AbC to the capture of Cu^{2+}, the S1/AuE without grafting of AbC was also immersed in Cu^{2+} solution and then electrochemically measured. It is found that the electrochemical response of Cu^{2+}-S1/AuE (curve b) is significantly weaker than that of Cu^{2+}-AbC-S1/AuE (curve c), suggesting that only small amount of Cu^{2+} was attached on the surface of S1/AuE. Additionally the electrochemical signal at this electrode is not stable during tests, which might be related to the dissociation of Cu^{2+}-S1 due to the weak electrostatic adsorption of Cu^{2+} with the phosphate group and/or carboxyl group on the MB probe. Moreover, it is found that when AbC was applied as the loading platform of Cu^{2+}, the redox potential of the electrode shows significant positive-shift in comparison with that of Cu^{2+}-S1/AuE, which can be explained by the environment difference of the electroactive center (Cu^{2+}) at these two electrodes: For Cu^{2+}-S1/AuE, because the small amount of attached Cu^{2+} ions is directly bound with phosphate group and/or carboxyl group of S1, they show larger freedom to get close to the electrode surface for electron transfer, and therefore a low redox potential was generated. In contrast, when Cu^{2+} was bound with AbC and then grafted to probe DNA, the Cu^{2+} is surrounded by the hydrophobic ring of AbC, thus the electrochemical reaction of Cu^{2+} at the electrode surface become difficult, making the redox potential of electrode shift in a positive direction. Therefore, from the difference of peak currents and peak potentials of the two electrodes, it can be concluded that that AbC is capable of functioning as an effective Cu^{2+} capturing platform for the construction of the electrochemical biosensing interface.

<Fig. 3 >

The electrochemical signals of the other common electroactive metal ions such as Co^{2+}, Sm^{3+}, Mn^{2+}, Fe^{3+} and Ni^{2+} after assembled on AbC-S1/AuE were also investigated. Fig. S-2 summarizes the peak currents of all the electrodes obtained in potential range from –0.2 V to 0.6 V, from which the bases of the probe DNA could be well protected from oxidation damage (Habibi et al. 2016; Yari et al. 2016). Clearly, the Ni^{2+}- and Mn^{2+}-incubated electrodes do not reveal any electrochemical response. The responses of Fe^{3+}, Co^{3+} and Sm^{3+} ions-modified AbC-S1/AuE are far lower than that of Cu^{2+}. These differences should be ascribed to strong coordinative ability of Cu^{2+} with the carrier platform of AbC and the higher electron-transfer kinetic and electrochemical stability of the Cu^{2+}-based tag (Chen et al. 2015; Drewry et al. 2011; Sharma et al. 2017).

Fig. 3B shows the CVs of the Cu^{2+}-assembled electrode at different scan rate (v) from 10 to 450 mV s^{-1}. As seen, the redox peaks on the electrode gradually grow as the scan rate increases. The oxidation peak currents (I_{pa}) present good linear relationship with the scan rate (v) as shown in the inset of Figure 3B. The regression equation is I_{pa} (μA) = –0.999–0.0116 v (mV s^{-1}) with correlation coefficient (r)= 0.993. This result indicates that the electron transfer reaction of Cu^{2+}/Cu^{+} on the fabricated sensing interface involves an surface adsorption-controlled process (Laviron et al. 1979), confirming that the electroactive Cu^{2+} has been anchored on the electrode-confined AbC-S1 layer.

3.3 Optimization of the experimental conditions

In order to achieve the optimal electrochemical response of the biosensor, some conditions for preparing the biosensor was optimized. Firstly, the accumulation time (t_a) of Cu^{2+} was optimized through immersing AbC-S1/AuE into 6.0 mM $Cu(NO_3)_2$ solution for different time, and then electrochemically measured in blank supporting solution after washing. Fig. 4A displays the relationship of oxidation peak currents (I_{pa}) with the time (t_a), from which it can be observed that the values of I_{pa} increase dramatically in the first 30 min and then hardly changed, suggesting the binding equilibrium between Cu^{2+} and AbC was accomplished within 30 min. Therefore, we chose 30 min as the optimal reaction time of Cu^{2+} on AbC-S1/AuE in this experiment.

Then, since Cu^{2+} can absorb on the phosphate backbone of probe DNA via the non-specific electrostatic interaction, unstable and large background response will be

generated during analysis application for the biosensor. In order to avoid this disadvantage, the electrode after absorbed with Cu^{2+} was further immersed into a buffer with high ion-strength buffer (10.0 mM PBS, 25.0 mM KCl and 0.10 M $MgCl_2$) to elute the electrostatically bound Cu^{2+}. Fig. 4B shows the effect of elution time (t_e) on oxidation peak currents (I_{pa}) of the biosensor. Obviously, the I_{pa} values decrease with the extension of t_e, and when the time is upon 30 min, the value of I_{pa} doesn't attenuate anymore, indicating that the un-coordinated Cu^{2+} have been removed from the electrode surface. Therefore, 30 min is chosen as the optimal elution time to eliminate the electrochemically adsorbed Cu^{2+} during fabricating the biosensor.

<Fig. 4 >

3.4 Analytical performance of the biosensor

The sensitivity of the biosensor was investigated by varying the concentration of the complementary target sequence (S2) ranging from 0.10 pM to 1.0 nM. Under the optimal conditions, the Cu^{2+}-AbC-S1/AuE was first incubated in hybridization buffer solution containing the different concentrations of S2 for 45 min at 37 °C. Then, the electrochemical measurements were operated in the supporting electrolyte via DPV. It is found that the DPV response remains basically unchanged until the concentration of S2 is up to 0.1 pM, and then, with increase of target DNA concentration in the hybridization buffer solution, the oxidation peaks of biosensor decrease accordingly (Fig. 5A). This can be ascribed to the configuration change of the MB probes (S1) from the loop-stem structure to the rigid linear configuration that induced by the hybridization reaction (Fan et al. 2003; Tanja et al. 2010).

The oxidation peak current changes ($\Delta I_{pa}=I-I_0$, where I is the peak current after hybridization and I_0 is the peak current before hybridization) of Cu^{2+}/Cu^{+} couple logarithmically relate to the target DNA (S2) concentrations across the range from 0.10 pM to 0.50 nM (inset of Fig. 5A), with a regression equation of ΔI_{pa} (μA) = 3.879 + 0.297 lg(C_{S2}/M), r=0.993. The detection limit was then estimated to be 0.060 pM based on the signal-to-noise characteristic (S/N=3). The analytical performance of the developed biosensor to CaMV 35s fragment was also compared with other sensing system, and the comparative results are listed in Table S-1 in Supporting Information. The result clearly shows that the analytical strategy presented in this work that obtained through the facile in-situ assembly of signal probe has the comparable and

even better analytical performance than the other methods, which can be explained by excellent electroactivity of Cu^{2+}-AbC tag and high hybridization efficiency of the unique stem-loop structured MB probe.

The selectivity of the developed electrochemical DNA biosensor was investigated through comparing the electrochemical results of the biosensor upon hybridization with complementary sequence (S1), one-base mismatched sequence (S3) and non-complementary sequence (S4). Fig. 5B shows the DPVs and the corresponding histogram (inset) of the oxidation peak current (I_{pa}) of Cu^{2+}-AbC-S1/AuE before (curve a) and after hybridization with S4 (curve b), S3 (curve c) and S2 (curve d). It is obviously observed that the signal difference between Cu^{2+}-AbC-S1/AuE and Cu^{2+}-AbC-S4-S1/AuE is negligible, suggesting that the hybridization reaction did not happened between S4 and S1 due to absolute base mismatching. After hybridization with S3, the oxidation peak decreases slightly, suggesting that the one-based mismatched DNA cannot effectively trigger the complete change of loop-stem structure of probe DNA to the linear form. However, when the biosensor was hybridized with totally complementary sequence of S2, the electrochemical responses decrease significantly. These results indicate that the probe DNA after assembly with AbC-Cu^{2+} complex still remains excellent hybridization selectivity.

<Fig. 5 >

3.5 Reusality, reproducibility and stability of the biosensor

The reproducibility of the biosensor was monitored by five parallel-made DNA biosensors to detect 0.50 nM target DNA and a relative standard deviation (RSD) of 8.5% (n=5) was estimated, illustrating that the developed biosensor has acceptable reproducibility. The regeneration of this DNA biosensor was performed by heating the hybridized electrode in 50 mM NaCl solution at 70 °C for 10 min, followed by a rapid cooling in an ice bath for 5 min. It is found that after five hybridization-regeneration cycles, the response of the prepared biosensor shows only about 5% loss of the original signal, presenting a satisfactory reusality. In addition, the stability experiments reveal that the fabricated biosensor shows the negligible signal changes after storing at 4 °C for 4 weeks, revealing a high stability, which can be ascribed to the high chemical stability of assemblied AbC-Cu^{2+} and excellent electrochemical reversibilty of the Cu^{2+}/Cu^{+}.

3.5 Determination of CaMV 35s fragment in soybean sample

The CaMV 35s promoter has been widely used to initiate transgene expression in many tissues and crop species. Therefore, the presence of CaMV 35s promoter is often regarded as a marker of genetically modified organisms (GMOs). In this work, in order to probe the feasibility and capability of the developed biosensor in real samples, the recovery assays were carried out in the complex matrices obtained from market-purchaced soybean. The detailed extraction and digestion procedures are given in section 2.5. The analytical results are displayed in Table 1. As seen, no CaMV 35s fragment was detected in the extracted sample, suggesting that the soybean is non-transgenic product. Then, when 1.00 pM, 10.0 pM, and 50.0 pM of CaMV 35s-related target DNA were respectively added into the complex matrices and then tested, the recoveries are in the range of 96.4-102.0%. For each sample, the RSDs are 3.6-5.2% with five parallel tests. These observations substantially demonstrate that the method can be potentially used for the detection of CaMV 35s in real samples.

<Table 1>

4. Conclusions

A novel DNA biosensor was facilely fabricated through stepwise in-situ labeling of AbC and Cu^{2+} on the free terminal of the hairpin-structured MB probe. The proposed strategy for the biosensor fabrication realizes the simultaneous label-separation-purification procedure, which is more time and labor-saving than the traditional method. The DNA biosensor has the advantages of high selectivity due to the unique stem-loop structure of the probe DNA. The oxidation peak currents presented a good linear relationship with the concentration of the target DNA from 0.10 pM to 0.50 nM. The developed DNA biosensor was satisfactorily applied to quantitatively detect the target DNA in real samples. This approach also shows immense talent in aptasensor and immurosensor construction, which can potentially become a convenient tool for specific sequence detection of genetically modified organism.

Acknowledgments

The work is supported by the National Natural Science Foundation of China (No. 21275127), Education-Science Research Project for Young and Middle-aged Teachers of Fujian (No. JA14195, JA15305 and JA15314).

References

Alves-Balvedi, R. P., Caetano, L. P., Madurro, J. M., Brito-Madurro, A. G., 2016, Biosens. Bioelectron. 85, 226-231.

Banyay, M., Sarkar, M., Gräslund, A., 2003. Biophys. Chem. 104, 477-488.

Chatelain, G., Ripert, M., Farre, C., Ansanay-Alex, S., Chaix, C., 2012. Electrochim. Acta 59, 57-63.

Chen, J., Huang, B. B., Zhan, S. Z., Ye, J. S., 2015. J. Electroanal. Chem. 759, 194-200.

Cui, H. F., Xu, T. B., Sun, Y. L., Zhou, A. W., Cui, Y. H., Liu, W., Luong, J. H. T., 2015. Anal. Chem. 87, 1358-1365.

Drewry, J. A., Gunning, P. T., 2011. Coord. Chem. Rev. 255, 459-472.

Diao, P., Guo, M., Jiang, D. L., Jia, Z. B., Cui, X. L., Gu, D. P., Tong, R. T., Zhong, B., 2000. J. Electroanal. Chem., 480, 59-63.

Fan, C. H., Plaxco K. W., Heeger A. J., 2003. PNAS 100, 9134-9137.

Fu, W., Wang, H. Y., Wang, C. G., Mei, L., Lin, X. M., Han, X. Q., Zhu, S. F., 2016. Biosens. Bioelectron. 77, 702-708.

Giambattista, L. D., Pozzi, D., Grimaldi, P., Gaudenzi, S., Morrone, S., Castellano, A. C., 2011. Anal. Bioanal. Chem. 399, 2771-2778.

Gokel, G. W., Leevy, W. M., Weber, M. E., 2004. Chem. Rev. 104, 2723-2750.

Habibi, B., Jahanbakhshi, M., 2016. Mikrochim. Acta 183, 2317-2325.

James, A. C., Kevin, W. K., Diep, V. C., 2004. J. Solid State Electr. 8, 722-726.

Kjällman, T. H. M., Peng, H., Soeller, Ch., Travas-Sejdic, J., 2010. Analyst 135, 488-494.

Laviron, E. 1979. J. Electroanal. Chem. 101, 19-28.

Lipp, M., Brodman, P., Pietsch, K., Pauwels, J., Anklam, E., 1999. J. AOAC Int. 82, 923-928.

Malothu, R., Jogayya, K. N., Kiran D. K., Pratyusha K., 2016. J. Med. Plant. Res. 9, 1098-1102.

Manzanares-Palenzuela, C.L., Martín-Fernández, B., Sánchez-Paniagua, López M., López-Ruiz, B.. 2015. TrAC-Trends Anal. Chem. 66, 19-31.

Mehta, V. N., Solanki, J. N., Kailasa, S. K., 2014. Mikrochim. Acta. 181, 1905-1915.

Mircescu, N. E., Oltean, M., Chiş, V., Leopold, N., 2012. Vib. Spectrosc. 62, 165-171.

Nowicka, A., Sliwinska, E., Grzebelus, D., Baranski, R., Simon, P. W., Nothnagel, T., Grzebelus, E., 2016. Sci. Hortic. 209, 132-138.

Park, I. H., Park, K. M., Lee, S. S., 2010. Dalton Trans. 39, 9696-9704.

Obradovic, M., Pasternak, J. A., Ng, S. H., Wilson, H. L., 2016. J. Microbiol. Methods. 126, 60-66.

Sharma, V. V., Tonelli, D., Guadagnini, L., Gazzano, M., 2017. Sens. Actuators B Chem. 238, 9-15.

Tyagi, S., Bratu, D. P., Kramer, F. R., 1998. Nat. Biotechnol. 16, 49-53.

Tabrizi, M. A., Shamsipur, M., Farzin, L., 2015. Biosens. Bioelectron. 74, 764–769.

Wang, J., Cai, X. H., Rivas, G., Shiraishi, H., Farias, P. A. M., Dontha, N., 1996. Anal. Chem. 68, 2629-2634.

Wang, T., Zheng, Z., Zhang, X. E., Wang, H., 2016. Talanta 158, 179-184.

Wang, Q. X., Ding, Y. T., Wang, L. H., Ni, J. C., Yu, Z. L., Lin, H. B., Gao, F., 2013. Chem. Asian

J. 8, 1455-1462.

Wang, Q. X., Gao, F., Ni, J. C., Liao, X. L., Zhang, X., Lin, Z. Y., 2016. Sci. Rep. 6, 22441.

Wang, Y., Liu, Y. Y., Han, J., Wang, L., Chen, T., Ni, L., 2015. Anal. Methods 7, 2339-2346.

Yang, W. W., Lai, R. Y., 2012. Chem. Commun. 48, 8703-8705.

Yari, A., Derki, S., 2016. Sens. Actuators B Chem. 227, 456-466.

Yılmaz, Ü. T., Çalık, E., Uzun, D., Karipcin, F., Yılmaz, H., 2016. J. Electroanal. Chem., 776, 1-8.

Zheng, D. L., Wang, Q. X., Gao, F., Wang, Q. H., Qiu, W. W., Gao, F., 2014. Biosens. Bioelectron. 2014, 60, 167-174.

Zheng, J., Yang, R. H., Shi, M. L., Wu, C. C., Fang, X. H., Li, Y. H., Li, J. S., Tan, W. H., 2015. Chem. Soc. Rev. 44, 3036-3055.

Figure captions

Fig. 1. Schematic illustration of the fabrication process of the DNA biosensor using *in-situ* assembled AbC-Cu^{2+} as the electroactive tag.

Fig. 2. ATR-FTIR spectra of bare AuE (a) and S1/AuE (b), AbC-S1/AuE (c)

Fig. 3. (A) CVs of AbC-S1/AuE (a), Cu^{2+}-S1/AuE (b) and Cu^{2+}-AbC-S1/AuE (c) in 0.1 M supporting electrolyte. (B) CVs of Cu^{2+}-AbC-S1/AuE with different scan rates ((a-k): 40, 60, 80, 100, 150, 200, 250, 300, 350, 400, 450 mV s^{-1}) and the relationship of oxidation peak (I_{pa}) with the scan rate (v) (Inset).

Fig. 4. Relationship of oxidation peak currents (I_{pa}) with the accumulation time (t_a) of AbC-S1/AuE in 6.0 mM $Cu(NO_3)_2$ solution (A), and with the elution time (t_e) by 10.0 mM PBS (pH 6.8) with 25.0 mM KCl and 0.1 M $MgCl_2$ (B).

Fig. 5. (A) DPVs of the biosensor upon hybridization with (a) 0 M, (b) 0.1 pM, (c) 0.5 pM, (d) 1.0 pM, (e) 5.0 pM, (f) 10.0 pM, (g) 50.0 pM, (h) 0.10 nM, (i) 0.50 nM, and (j) 1.0 nM target DNA. Inset is the plot of peak current difference (ΔI_{pa}) versus the logarithm of the target DNA concentration (lg C_{S2}). (B) DPVs of Cu^{2+}-AbC-S1/Au before (a) and after hybridization with S4 (b), S3 (c) and S2 (d). Inset shows the corresponding histogram.

Table 1 Measurements of target DNA in the real samples obtained from market-purchased soybean using the developed method[a].

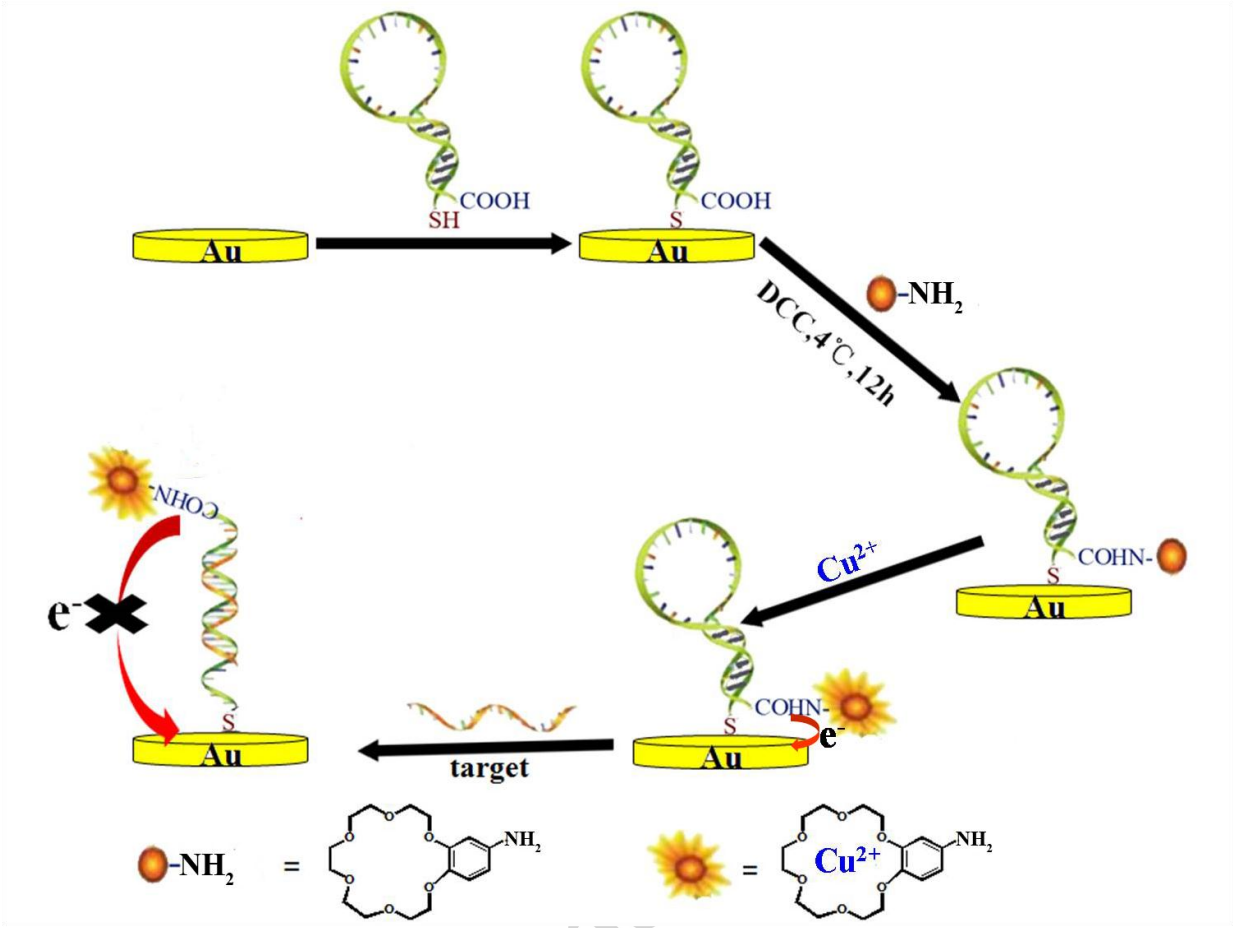

Fig. 1

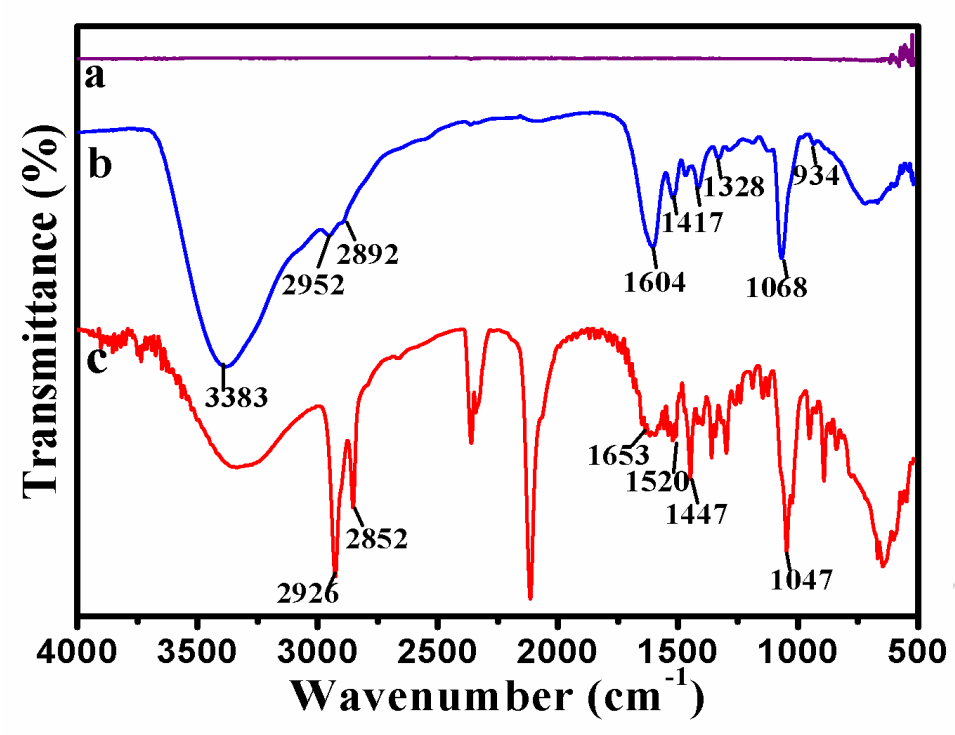

Fig. 2

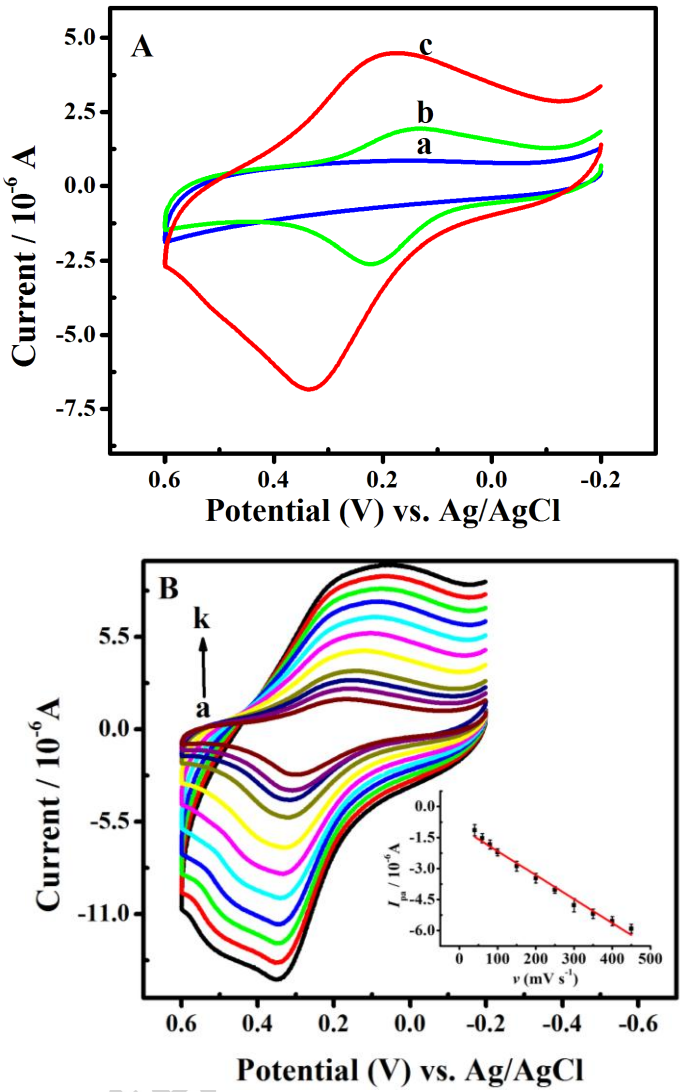

Fig. 3

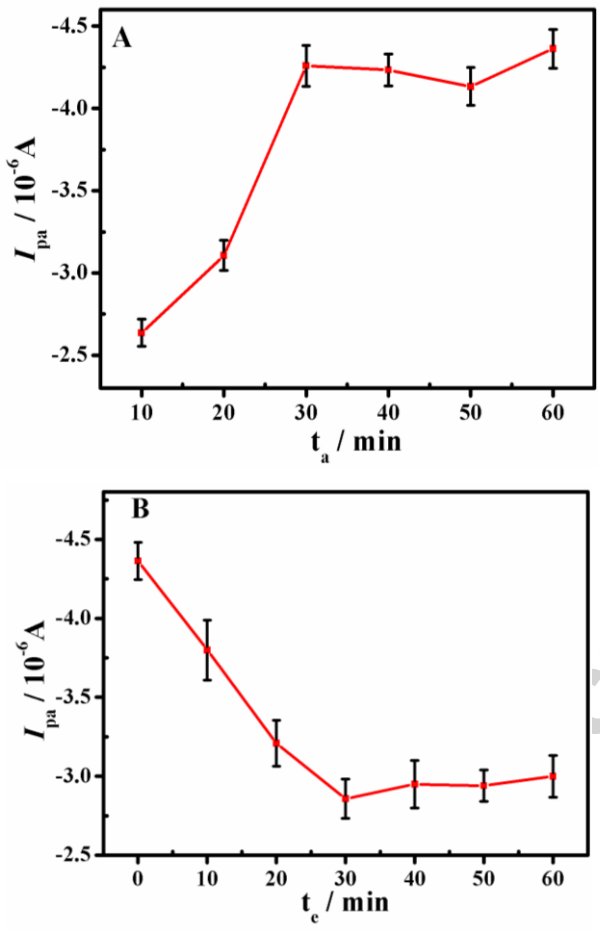

Fig. 4

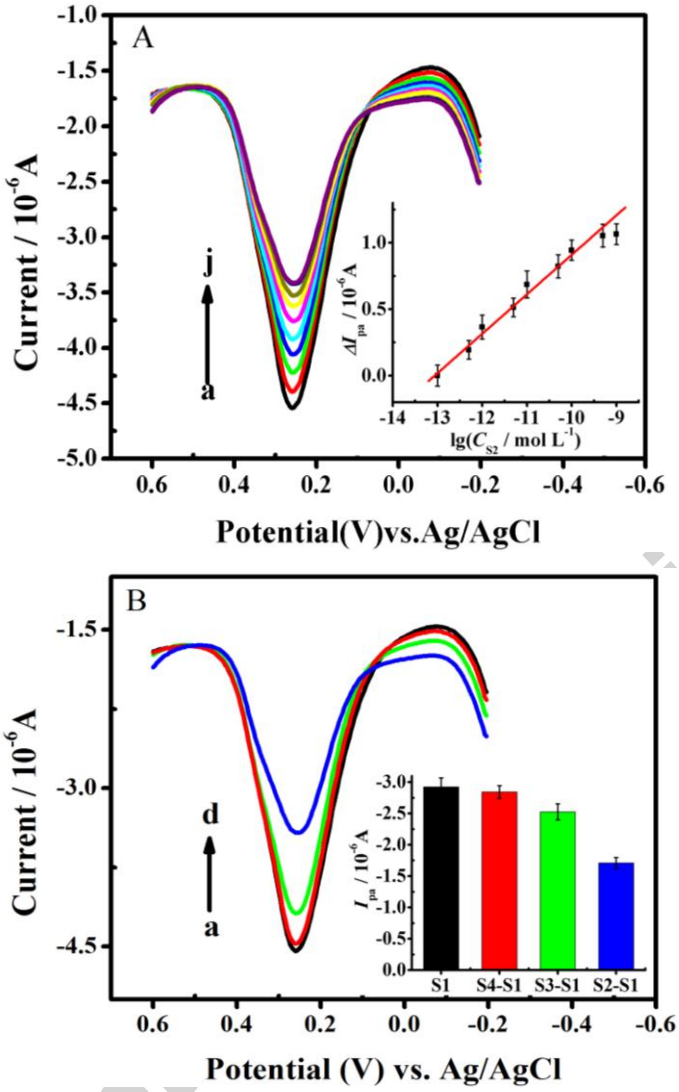

Fig. 5

Table 1 Detection of CaMV 35s in real samples extracted from soybean by the proposed biosensor[a].

Added	Found	Recovery (%)	RSD(%)
0	–	–	–
1.00 pM	(1.02±0.05) pM	102.0	4.3
10.0 pM	(10.1±0.03) pM	101.0	5.2
50.0 pM	(48.2±0.05) pM	96.4	3.6

[a]All values were obtained as an average of five repetitive determinations plus standard deviation

Highlights

► A molecular beacon-based biosensor was constructed using AbC-Cu^{2+} as signal tag.

► The tag was assembled on molecular beacon probe by in-situ modification approach.

► Linear range from 0.10 pM to 0.50 nM, and detection limit of 0.060 pM were achieved.

► The biosensor is capable of detecting CaMV 35s in soybean extraction sample.